

Fused Filament Fabrication, a new fabrication paradigm for 3D printing capacitive sensors: design, fabrication, and characterization for liquid level measurements.

Gianni Stano ^a, Attilio Di Nisio ^b, Anna Maria Lanzolla ^b, Mattia Ragolia ^b, Gianluca Percoco ^{*a}

^a Department of Mechanics, Mathematics and Management, Polytechnic of Bari, Via E.Orabona 4, 70125 Bari, Italy

^b Department of Electrical and Information Engineering, Polytechnic of Bari, Via E. Orabona 4, 70125 Bari, Italy

*Corresponding author: gianluca.percoco@poliba.it

Keywords: Additive Manufacturing, 3D printed capacitive sensors, multi-material printing, 3D printed liquid level measurement sensor, conductive filaments

Abstract

In recent years, the exploitation of Additive Manufacturing technologies for the fabrication of different kinds of sensors has abruptly increased: in particular, a growing interest for extrusion-based techniques has emerged. This research proposes the exploitation of Fused Filament Fabrication (FFF) process and two commercial materials (one flexible and one conductive) for the monolithic fabrication of a stretchable, coplanar capacitive sensor. The whole sensor, consisting of a flexible substrate and two electrodes, has been fabricated in a single-step printing cycle: Design for Additive Manufacturing approach was used, setting out a methodology to direct 3D print thin and close tracks with conductive materials, in order to obtain high capacitance values measurable by common measurement instrumentations.

Despite a huge exploitation of FFF technology for piezoresistive-based sensors, this manufacturing process has never been used for the fabrication of coplanar capacitive sensors since the manufacture of thin and close conductive tracks (key requirement in coplanar capacitive sensors) is a challenging task, mainly due to low manufacturability of extruded conductive beads with a high level of detail. Two versions of the sensor were developed: the first one with an embedded 3D printed coverage (ready to use) and the second one which requires a further manual post-processing to seal the electrodes.

The main benefits related to the exploitation of FFF technology for these sensors are: *i)* the reduction of the number of different manufacturing processes employed, from at least two in traditional manufacturing approach up to one, *ii)* the exploitation of a cost-effective technology compared to traditional high-cost technologies employed (i.e. lithography, inkjet etc.) *iii)* the reduction of manual and assembly tasks (one of the proposed versions does not require any further task) , and *iv)* the cost-effectiveness of the sensors (in a range between 0.27 € and 0.38 €).

The two developed prototypes have been tested demonstrating all their potentialities in the field of liquid level sensing, showing results consistent with the ones found in scientific literature: good sensitivity and high linearity and repeatability were proved when different liquids were employed. These 3D printed liquid level sensors have these features: *i)* flexible sensor, *ii)* the length is limited only by the machine workspace, *iii)* they can be either applied outside of the traditional reservoirs or embedded into the reservoirs (by 3D printing both the reservoir and sensor in the same manufacturing cycle), and *iv)* simple calibration.

Finally, the stretchability of these sensors paves the way toward their application for liquid level sensing into tanks with non-conventional shapes and for other application fields (i.e. soft robotics, non-invasive monitoring for biomedical applications).

1. Introduction

Recently, a growing interest in 3D printed sensors manufactured by means of extrusion-based Additive Manufacturing (AM) processes has emerged [1]; in particular, fused filament fabrication (FFF) technology, due to several intrinsic features (i.e. cheap technology, multi-material printing etc.), seems to be very promising for sensor manufacturing. Several advances have been carried out in the exploitation of multi-material FFF for this purpose: Arh et al [2] proposed an experimental method to identify the dynamic piezo resistivity of unidirectionally printed structures providing coefficients needful for the building of analytical and numerical models; Cardenas et al [3] used high intensity pulsed light to increase of two orders of magnitude the conductance of the tracks made up of commercial conductive filaments; Stano et al [4], taking advantage from Design of Experiment (DoE) tool, found a relationship between process parameters (layer height and printing orientation) and electrical resistance and variability minimization; Maurel et al [5] defined a novel framework to direct 3D print ion-lithium battery. As well outlined in [6], FFF technology is almost exclusively used to manufacture sensors based on piezoresistive principle, ranging from classic applications such as static load detection [7], [8] up to dynamic load detection [9] which motivates Arh et al [10] to develop a novel monolithic uniaxial accelerometer. A not negligible aspect related to FFF-made resistive sensors concerns the strong dependence between resistance change and temperature change, since the mechanism underlying this phenomena is not fully understood in literature and more research efforts are necessary to better characterize it: at the state of the art, the exploitation of these sensors to detect a change in temperature seems to be still not possible due to a low repeatability [11]–[13], [4].

Although a massive research in the field of multi-material FFF aimed to resistive sensors, this kind of AM technology is still today underexploited for the fabrication of capacitive sensors: in 2021, Loh et al [14] proposed the first capacitive-based force sensor entirely manufactured through FFF technology. Stretchable capacitive sensors are gaining a lot of interest in several application fields (i.e. sensing of liquid level, humidity, and temperature, motion detection etc.) and generally they are fabricated using at least 2 different manufacturing technologies: one for the flexible substrate and one for the electrodes. At the state of the art, non-AM processes such as lithography, spin coating, moulding etc. are employed for substrate fabrication, whereas AM technologies are often involved in the manufacture of the electrodes (some more non-AM technologies used for the electrodes are spray deposition, flexography, gravure, screen printing etc. [15]). The employed AM processes (generally inkjet in all its variants, Aerosol Jet micro-additive manufacturing, etc.) are expensive and often custom-made conductive materials (inks) are required due to a lack on the market [16]–[20].

In the present paper, an innovative manufacturing process was proposed based on the use of multi-material FFF technology to manufacture a stretchable, coplanar, capacitive sensor in a monolithic way: two commercial filaments (one flexible and one conductive) have been employed to fabricate the whole sensor in a single-step printing cycle. In this way, only one manufacturing process has been involved and no manual assembly tasks have been required, leading to a considerable reduction of cost, time and supply chain. Two versions of the sensor have been manufactured; afterwards, several characterization tests have been carried out proving the potentialities of the proposed sensors in the field of liquid level sensing. The paper is structured as follows: in section 2, the design and manufacturing details are provided; in section 3 all the characterization tests are summarized and discussed. Finally, conclusions are drawn in section 4.

2. Design and Manufacturing

The main reason of the low exploitation of FFF multi-material approach to the monolithic fabrication of stretchable coplanar capacitive sensor lies in the difficulty to print, with this technology, conductive tracks with a high level of details, that is very thin tracks and really close each other. Low detail levels are related to low capacitance, which is difficult to be measured by common measurement instrumentations. To obtain thin and close tracks, i.e. high capacitance, the Design for Additive Manufacturing (DfAM) approach was used, and several considerations have been pointed out, in order to overcome some typical issues related to the extrusion of conductive filaments.

Two versions of the sensor were manufactured: the main difference between them concerns the top coverage (in the first version it is missing, whereas in the second one it is embedded).

2.1 Design

Two versions of the capacitive, coplanar sensor were designed and manufactured: the first version named “Uncovered” consists of a flexible substrate and two coplanar electrodes, the second version named “Covered” consists of the same two elements of the first one more a top coverage which seals off the electrodes. Basically, after the manufacturing, the “Covered” sensor, is ready to be used, the “Uncovered” sensor, instead, needs a further manual task: a sealing adhesive tape was glued on the top of the sensor to isolate the top electrodes from the surrounding environment.

All the elements shared by the two versions are characterized by the same dimensions. The substrate dimensions are 55 mm and 171 mm along x- and y-axis (see Fig.1), while the width of the substrate is 0.4 mm.

The design of the electrodes is a crucial point to obtain a measurable capacitance value. In fact, the thinner and closer the electrodes, the higher the capacitance is, but, at the same time, technological (FFF) constraints must be taken into account when conductive filaments are extruded. In accordance to [16] the capacitance of the coplanar capacitive sensors is defined by the following equation:

$$C = Nl\varepsilon_0\varepsilon_{ea} \frac{K(\sqrt{1 - k_0^2})}{K(k_0)} \quad (1)$$

where C (pF) is the capacitance of the whole sensor, N (dimensionless) is the number of electrodes pairs, l (mm) is the length of each electrode along x-axis, ε_0 is the vacuum dielectric constant ($\frac{pF}{mm}$), ε_{ea} (dimensionless) is the effective dielectric constant of capacitive sensor in the air (further details

about this parameter are well explained in [16]), and $K(k_0)$ (dimensionless) is the elliptical integral of the first kind in terms of k_0 , where k_0 is defined as follows

$$k_0 = \frac{s}{s + 2w} \quad (2)$$

where s (mm) and w (mm) are the electrodes spacing and width, respectively.

Thus, the only design parameters that can be set in order to maximize the final capacitance are N , l , s and w (see Fig.1).

As a matter of fact, the free design variables are the l parameter (length of the single electrode along x-axis) and the active electrodes length (along y-axis), which have been suitably set as 25 mm and 150 mm, respectively. Consequently, considering all the manufacturing constraints (detailed in section 2.1), it was found that the best N , s and w values to maximize the final capacitance were 57, 0.8 mm and 0.4 mm, respectively.

In particular, the DfAM approach was used to successfully set w : considering the printing orientation (sensor flat over the build plate with flexible substrate in contact with it), w parameter depends on the line width process parameters, which in turn depends on the dimension of the nozzle. From equation (1), the need to minimize w stands out, but this is in contrast with the processability of the conductive materials (the bigger the nozzle, i.e. from 0.6 mm up to 1 mm, the less are the printing issues such as filament breakdown and clogged nozzle): by setting further process parameters (detailed in Section 2.2) it has been possible to use a 0.4 mm nozzle and set $w = 0.4$ mm, i.e. a single extruded line. Similar considerations can be drawn for the s parameter: using a trial-and-error approach it was found that the minimum spacing between two adjacent electrodes lines allowed by FFF machine for the conductive material and the 0.4 mm nozzle was 0.8 mm, lower values involved contamination (contact) among adjacent electrodes. The height of the electrodes was arbitrarily set as 0.8 mm, however lower values are allowed.

All the above mentioned features are common to both the “Uncovered” and “Covered” versions; the latter, in addition, presents a 0.3 mm thick top cover over the electrodes made of the same material, i.e. thermoplastic polyurethane, used for the flexible substrate (see Fig.2). Moreover, both sensors were equipped with two square pads (side equal to 10 mm) to weld electrical wires, to connect the sensors to a benchtop digital multimeter or a read-out circuit.

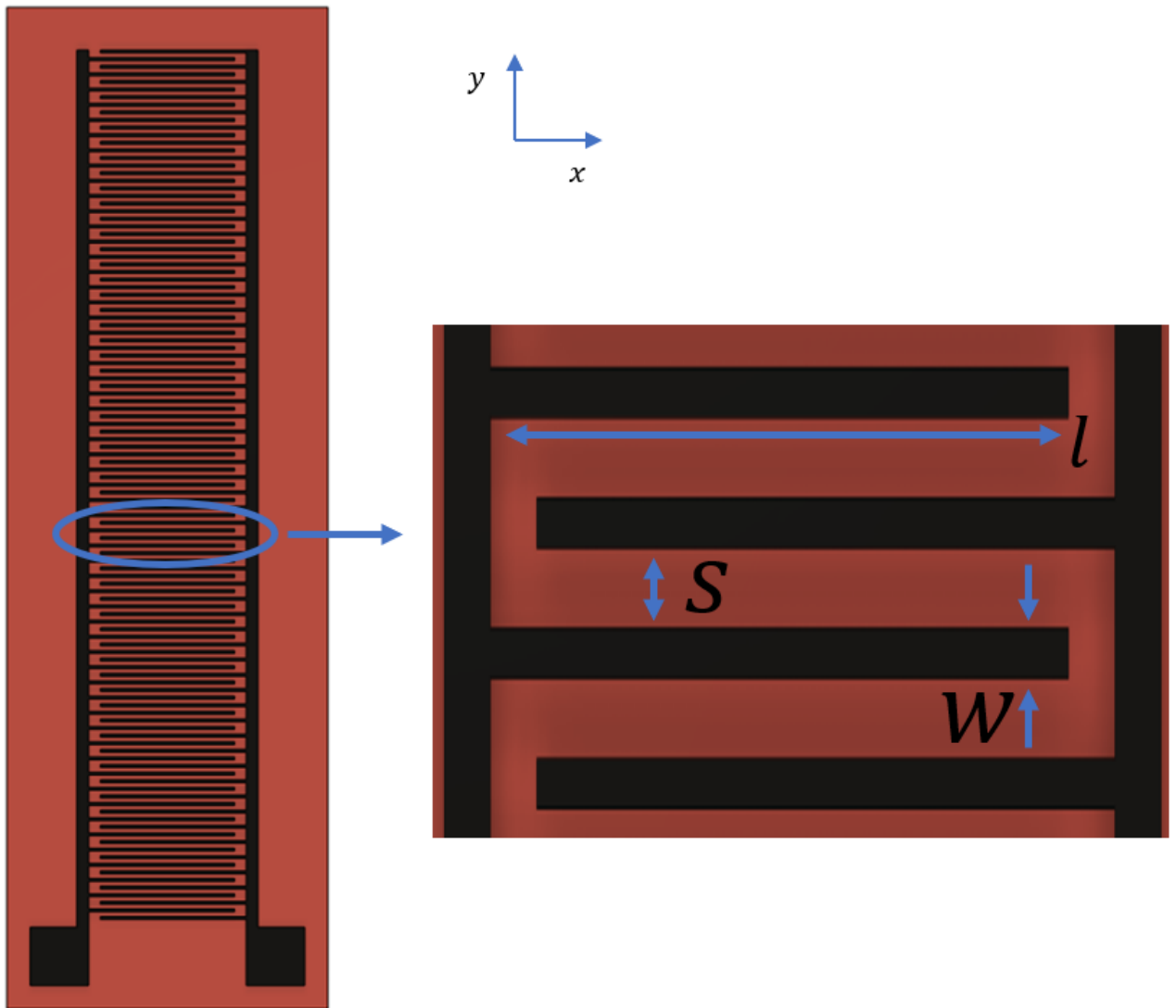


Figure 1- Design of the coplanar capacitive sensor, in red the flexible substrate and in black the two electrodes (this image refers to the “Uncovered” version).

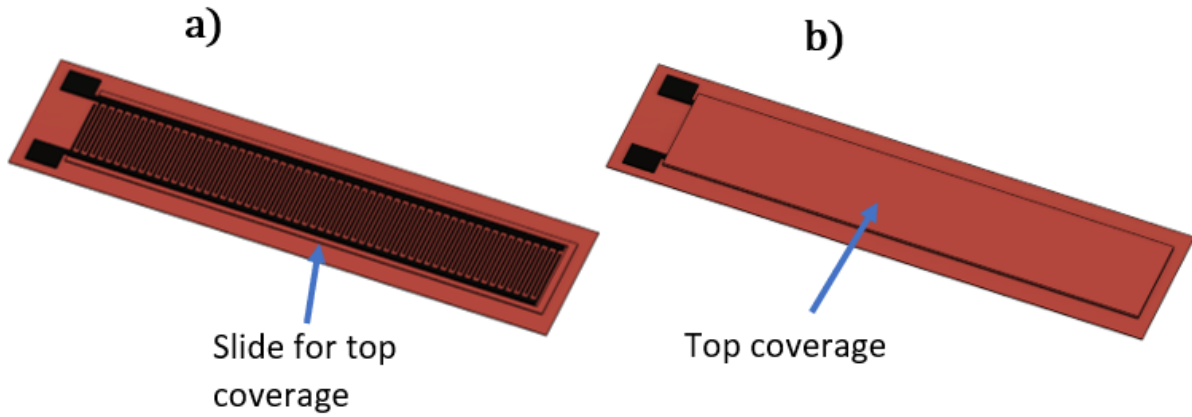


Figure 2- “Covered” sensor- a) the lateral slide made of flexible thermoplastic polyurethane on which the top coverage will be manufactured is shown, b) final sensor with the 0.3 mm top coverage.

2.2 Additive Manufacturing

The two versions of the sensor have been fabricated in a monolithic way, exploiting the advantages of the FFF technology. A multi-material FFF 3D printer (Ultimaker 3, Ultimaker, Netherland) and two commercial materials were used. For the flexible substrate (and top coverage of “Covered” version) a commercial flexible thermoplastic polyurethane was employed, namely the red color Ultimaker TPU, with shore A hardness equal to 95 (henceforth called TPU), characterized by a tensile modulus of 26 MPa and an elongation at break of 580%; whereas for the electrodes a commercial conductive polylactic acid (PLA)- based filament was employed, doped with carbon black and carbon nanotubes (CNTs), and characterized by a resistivity of $15 \, \Omega \cdot \text{cm}$ along the layers and $20 \, \Omega \cdot \text{cm}$ perpendicular to the layers, namely the AlfaOhm by FiloAlfa (Italy) henceforth called AlfaOhm. All technical data are reported on the data sheets of that materials. For TPU and AlfaOhm, 0.8 mm and 0.4 mm nozzles were used, respectively.

As a matter of fact, the smaller the nozzle size is, the more the level of detail is: when conductive materials (generally PLA-based doped with CNTs) are used, the general advice provided by filaments suppliers is to use nozzles with dimensions larger than 0.6-0.8 mm. The main problem which could occur when nozzles smaller than 0.6 mm are employed is the filament breakdown between the gears which push it into the extruder; in fact, the doping elements (i.e. CNTs) make the filament very brittle.

As demonstrated in Percoco et al [21] in 2021, the reduction of the total force (inside the nozzle + counterpressure) is the key to overcome filament breakdown between the gears: by reducing the total printing force, the pushing force of the gears on the conductive filament will be reduced too. The main process parameters affecting the total force are layer height and printing temperature: when they increase, the total printing force decreases. Both these process parameters are the key enablers to

obtain high level of details with a brittle filament such as TPU doped with carbon nanoparticles and nanotubes, allowing the exploitation of 0.4 mm nozzle. Hence, in this case the exploitation of 0.4 mm nozzle is allowed by setting the layer height parameter as 0.2 mm, unlike the classic printing scenario, in which high details are reached setting a low value of layer height (i.e. 0.05 mm) [22]. Moreover, the printing temperature of the conductive filament was set to 225 °C, higher than the suggested printing temperature range of 190-210 °C provided by the supplier. By setting the above mentioned process parameters (layer height as 0.2 mm, and printing temperature as 225°C), it has been possible to use 0.4 mm nozzle and create electrodes with a width (w parameter in section 2.1) equal to the nozzle diameter, i.e. 0.4 mm, without any filament breakdown despite a huge number (more than 20) of consecutive printed sensors.

In Tab.1 the main process parameters for both the materials are summarized.

The total cost of the “Uncovered” and “Covered” sensor, estimated by the slicer (Ultimaker Cura 4.6) was 0.27 € and 0.38 €, while the printing time was 42 minutes and 56 minutes.

Figure 3-a) shows the proposed sensor during the 3D printing.

Table 1- Process parameters

	TPU	AlfaOhm
Nozzle size (mm)	0.8	0.4
Layer height (mm)	0.2	0.2
Printing temperature (°C)	223	225
Line width (mm)	0.8	0.4
Printing speed (mm/s)	30	25
Flow (%)	106	110

The core difference between “Covered” and “Uncovered” sensor is that the first one can be employed without recurring to any further post-processing, while the second one needs to be sealed in order to isolate the electrodes from the surrounding environment. For the “Uncovered” version, a common adhesive tape was manually glued on the top. A not negligible advantage of the “Covered” version concerns the total absence of the necessity to seal the electrodes, which may require further post-processing such as coating, often a manual task strongly related to operator’s skills [23], [24]. In Fig.4 the two manufactured versions are shown.

Another main benefit of these kinds of 3D printed capacitive sensors is their flexibility (see Fig 3-b)): they can be easily attached to irregular and non-conventional shapes paving the way for their exploitation in the field of the wearable sensors.

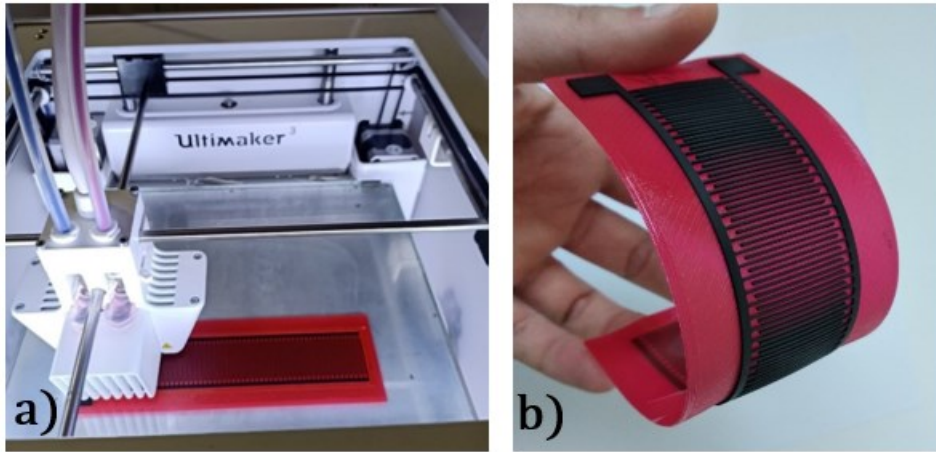


Figure 3- a) Capacitive sensor during the manufacturing process, b) flexibility of the sensor



Figure 4- Manufactured sensors; a) “Uncovered” sensor, before being sealed with adhesive tape and, b) “Covered” sensor with 0.3 mm top TPU cover.

Finally, to prove the manufacture method robustness, 10 samples of each version have been printed, carrying out the following conclusions: *i)* no filament breakdown occurred, and *ii)* for “Covered” and “Uncovered” versions, the mean capacitance value (calculated after the manufacturing and the manual tape attachment, respectively) was 0.1517 nF and 0.1542 nF with a very low standard deviation of 0.0007 nF and 0.001 nF respectively, due to not uniform electrical resistance of the raw conductive filaments (before of being melted into the nozzle) and noise effects occurring during the printing such as vibrations, room conditions etc.

3. Characterization

In this section, the two versions of the sensor were both tested as liquid level sensors, showing different behaviors under various aspects (i.e. sensitivity, offset etc.). Two different liquids were used to test the sensors, i.e., distilled water and sunflower oil. The measurement setup, shown in Fig.5, consists of:

- i.* a custom-made 3D printed tank, which presents a vertical channel in which was manually injected a constant quantity of liquid by means of a syringe. The vertical channel avoids the spatter of liquid droplets on the surface of the sensors, which could lead to errors in the liquid level measurement.
- ii.* a 34461A digital multimeter (Keysight Technologies, Santa Rosa, California, U.S), with 6 $\frac{1}{2}$ digits of resolution, for accurate measurements of capacitance in a range of 1 nF.
- iii.* a control program developed in LabVIEW® by National Instruments Corp., to easily manage the system, providing real-time monitoring and data storage for further processing.
- iv.* a digital scale with a resolution of 0.001g to measure the amount of liquid to inject.

The measurement protocol used to characterize the sensors for water and sunflower oil sensing is described in the underlying subsections.

Before performing experiments, a preliminary test was performed to prove the tightness of the top coverages when immersed in two different liquids. Firstly, “Covered” and “Uncovered” sensors were kept into a tank full of water for 48 h and no coverage degradation was observed for both the versions. Afterwards, the same test was performed using sunflower oil and a different behavior was observed only for “Uncovered” version: after about 20 minutes, the oil attacked the sealing adhesive tape and caused its detachment, leaving the electrodes directly exposed to the oil and consequently making the whole “Uncovered” sensor unusable.

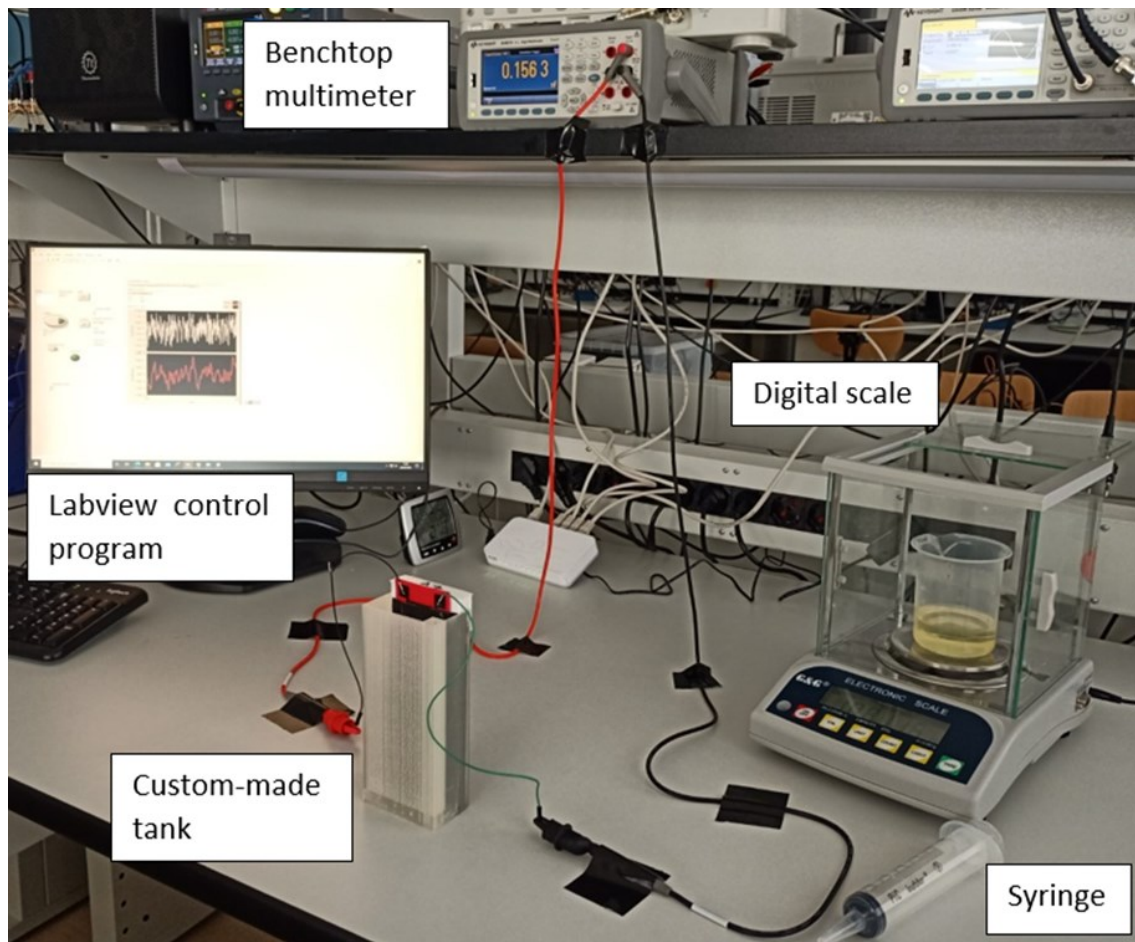


Figure 5- *Measurement setup.*

3.1 Water level sensing

“Covered” and “Uncovered” sensors were both tested for the sensing of distilled water level: several conclusions can be drawn highlighting the differences between the two versions and proving that their behavior is consistent with capacitive sensors described in scientific literature.

The same measurement protocol was used for both versions: the same quantity of liquid, weighed by means of the high accuracy digital scale, was injected into the tank 5 times (5 steps in total); at each step, a settling time of 30 s was waited from the injection of the liquid, and the average of 20 consecutive capacitance readings was computed, in order to reduce noise. Note that the quantity of liquid of the first step can slightly differ from the following ones: this does not affect the results, since it serves only for detecting the first measurable capacitance change after liquid injection. The whole procedure is repeated 10 times (a total of 10 test cycles) for each version of the sensor, to assess repeatability. After each test, a time sufficient to manually dry the sensor and to empty the tank was waited, less than 4 minutes.

Fig.6 shows the results for both versions of the sensor. It can be noted a high linearity of the sensitivity to the level of liquid, as common to capacitive level sensors found in scientific literature [16], [17], [24]. Sensitivity of “Uncovered” and “Covered” sensors are, respectively, $0.49 \pm 0.01 \frac{pF}{mm}$ and $0.79 \pm 0.01 \frac{pF}{mm}$ (mean \pm std), obtained by performing linear regression on each curve (with a mean coefficient of determination R^2 of 0.9988 and 0.9973, respectively) and by averaging the results of the 10 tests. “Covered” sensor presents a sensitivity about 60% higher than “Uncovered” sensor: as well explained in [16], the top cover of the sensor is accountable for the different sensitivity, in fact the main differences between the two top covers (embedded TPU cover and adhesive tape cover for “Covered” version and “Uncovered” version, respectively) are *i)* the cover thickness and *ii)* the dielectric constant of the cover material.

These results are very important: for example, if compared to [17], the proposed sensors present a sensitivity one order of magnitude higher, being manufactured in a monolithic way, using a much cheaper fabrication technology.

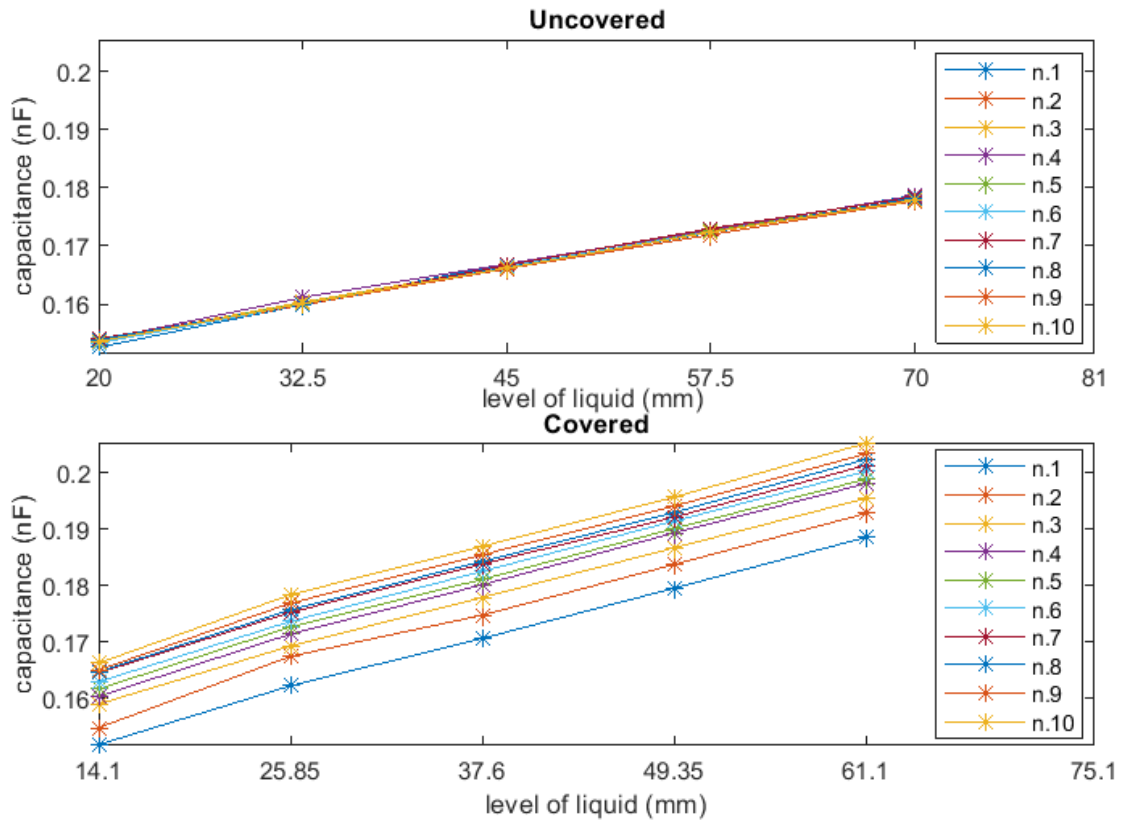


Figure 6 - Capacitance vs liquid level of distilled water level. The same scale is used for both x- and y-axis for better visualization and comparison.

Moreover, for each test performed on the “Covered” sensor, it could be noted an offset between each curve, whereas the curves of “Uncovered” sensor seem to be more overlapped. In order to better

investigate this phenomenon, Fig.7 shows the difference of the offset of each curve with respect to the first curve. “Uncovered” sensor presents a first offset of about 1.2 pF in the second curve; then, offsets assume a random distribution with mean and standard deviation of 1.42 ± 0.24 pF. In authors’ opinion this random offset could be due to *i)* changes in room conditions (i.e., slight temperature change), *ii)* changes in tank conditions (i.e. slight humidity change: in fact, after each test cycle the tank was manually cleaned up and some drops of waters could have been remained into the tank), and *iii)* slight changes in the position of connection wires.

“Covered” sensors, instead, presents increasing offset for each test, spanning a range up to 14.5 pF: compared to its counterpart, i.e. “Uncovered” version, the offset is meaningfully high (806 %) and is not random distributed but it is ever-growing. In addition to random variable changes, above described, in this case another important phenomenon takes place: the TPU material, of which the top cover is made, is characterized by a water absorption value of 0.18% in accordance with ASTM D570 test method (material data sheet). As a matter of fact, after each test cycle a certain amount of water gets trapped into the TPU cover leading to an ever-increasing initial capacitance value (initial offset) from test cycle n to $n+1$, with $n=1, \dots, 9$. This behavior was missing in “Uncovered” version because of the non-water absorption of the adhesive tape used to seal up the electrodes. Moreover, despite the increasing initial offset, the “Covered” version, characterized by a higher sensitivity compared to its counterpart, can be still employed by performing a zeroing procedure to compensate offset.

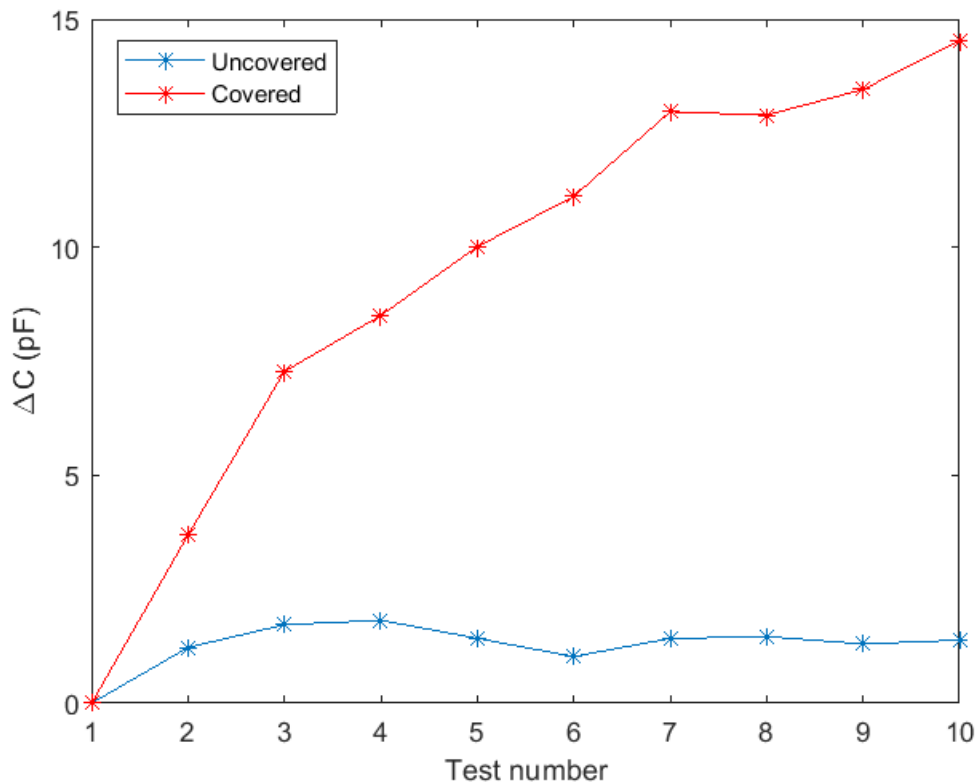


Figure 7 – Offset of linear regression curves with respect to the 1st one – distilled water.

Resuming, both versions can be employed as water level sensors:

- “Uncovered” version shows a sensitivity of $0.49 \pm 0.01 \frac{pF}{mm}$, a mean coefficient of determination R^2 of 0.9988 and a randomly distributed offset within a range of 1.8 pF, defined as random offset due to environmental conditions.
- “Covered” version shows a sensitivity of $0.79 \pm 0.01 \frac{pF}{mm}$, a mean coefficient of determination R^2 of 0.9973 and an ever-increasing offset spanning a range of 14.5 pF due to both random conditions (minimum contribution) and water absorption behavior of TPU top coverage (main contribution).

3.2 Oil level sensing

The tests in section 3.1 have been repeated for the sensing of sunflower oil level; the same measurement protocol was applied. Fig.8 shows the results for “Uncovered” and “Covered” sensors, respectively. For “Uncovered” version of the sensor, only 3 tests have been performed, because the oil caused the detachment of adhesive tape, thus directly touching the electrodes, making the sensor unusable (as explained in section 3)

As for water sensing, a high linearity is observed for both “Uncovered” and “Covered” sensors, which present a sensitivity of $0.069 \pm 0.002 \frac{pF}{mm}$ and $0.078 \pm 0.002 \frac{pF}{mm}$ (mean \pm std), respectively, obtained by performing linear regression on each curve (with a mean coefficient of determination R^2 of 0.9982 and 0.9977, respectively) and by averaging the results of each test. These values are, as expected, one order of magnitude lower than the ones obtained with distilled water, in fact sunflower oil is characterized by different electrical properties (a lower electrical conductivity and dielectric constant).

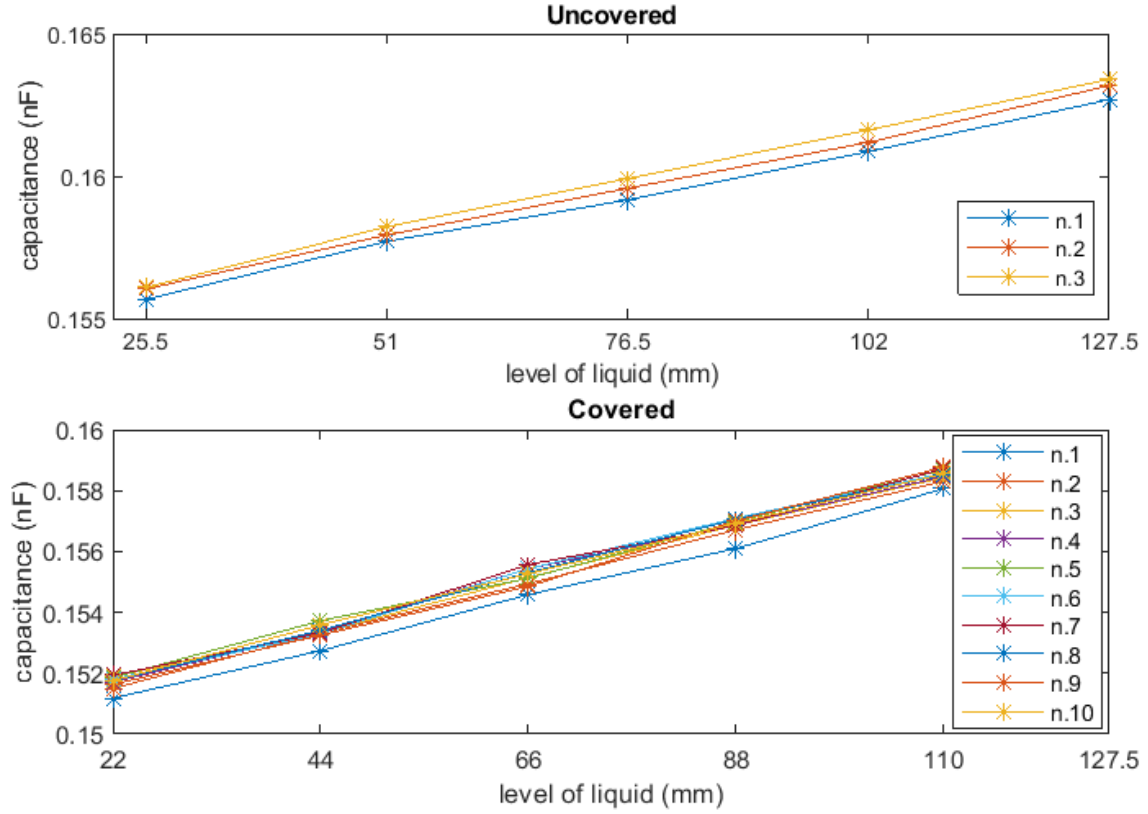


Figure 8 - Capacitance vs liquid level of sunflower oil. The same scale is used for both x- and y-axis for better visualization and comparison.

Unlike the tests presented in section 3.1, when sensing sunflower oil both “Uncovered” and “Covered” sensors present low offset (less than 1 pF) of the same order of magnitude of the offset in water sensing test with the “Uncovered” version (1.2 pF), previously described, and defined as random offset due to slight changes in room, tank and wire conditions.

The offset of the “Covered” version presents a random distribution, with mean and standard deviation of 0.64 ± 0.16 pF.

Finally, “Covered” sensor does not show increasing offset, as it was for water sensing. In fact, the employed TPU material does not provide any evidence of oil absorption, unlike for water.

Resuming, only “Covered” version can be employed as oil level sensor because of adhesive tape detachment of “Uncovered” version after 3 test cycles (about 20 minutes), making it unusable. “Covered” version was characterized by a sensitivity of $0.078 \pm 0.002 \frac{\text{pF}}{\text{mm}}$, a mean coefficient of determination R^2 of 0.9977 and a random offset less than 1 pF.

4. Conclusion

In the present paper the extrusion based fused filament fabrication (FFF) technology is employed, as a new manufacturing process for stretchable coplanar capacitive sensor. In literature, FFF is widely reported to manufacture piezoresistive sensors whereas it is still underexploited in the field of coplanar capacitive sensors. The main reason is that thin and close conductive tracks using commercial conductive materials are complex: the latter is a crucial requirement to achieve capacitance values measurable by the multimeters. Using a Design for Additive Manufacturing (DfAM) approach and setting a customized printing strategy, it was possible obtain the designed conductive tracks.

The main advantage in the exploitation of FFF concerns the possibility to manufacture the whole sensor, composed of a flexible substrate and two electrodes monolithically, in a single step printing cycle, using commercial materials, and avoiding the exploitation of several different manufacturing processes. Two versions of the sensor were developed and tested: one requires a further manual process to seal up the electrodes, while the other is composed by an embedded 3D printed top cover.

Resuming, from a manufacturing point of view, the following outcomes have been achieved:

- It has been manufactured a stretchable, coplanar capacitive sensor in a monolithic manner, by using flexible and conductive filaments in the same working cycle.
- Thin and close conductive tracks have been fabricated overcoming the classical breakdown issue which affects brittle conductive filaments by reducing the total printing force (setting high values of layer height and printing temperature parameters).
- The “Covered” version of the sensor is characterized by an embedded top TPU cover avoiding further post processing steps and, often, manual tasks (i.e. a coating process) required to isolate the electrodes.

Several considerations were carried out from characterization experiments: both sensors were tested for liquid level sensing (two different liquid were employed, namely water and oil) showing good sensitivity, high linearity (for each sensor and each liquid tested, a mean coefficient of determination R^2 more than 0.99 was observed) and high repeatability. In particular, the “Covered” sensor seems to be very promising for oil level sensing, overcoming the main problem related to the detachment of external sealing coverages.

In conclusion, the present work provides a methodology to monolithically fabricate stretchable, coplanar capacitive sensors with FFF, paving the way for a replacement of the traditional manufacturing technologies and an easy integration of these sensors into very complex structures fabricated in the same printing cycle, such as soft robots or tanks with non-conventional shapes for

liquid level sensing; furthermore, the non-invasive monitoring in biomedical field may also benefit from the proposed fabrication methodology.

References

- [1] M. Schouten, G. Wolterink, A. Dijkshoorn, D. Kosmas, S. S. Fellow, and Gijs Krijnen, “A Review of Extrusion-Based 3D Printing for the Fabrication of Electro- and Biomechanical Sensors,” no. AUGUST, pp. 1–12, 2020, doi: 10.1109/JSEN.2020.3042436.
- [2] M. Arh, J. Slavič, and M. Boltežar, “Experimental identification of the dynamic piezoresistivity of fused-filament-fabricated structures,” *Addit. Manuf.*, vol. 36, no. April, p. 101493, 2020, doi: 10.1016/j.addma.2020.101493.
- [3] J. A. Cardenas *et al.*, “Flash ablation metallization of conductive thermoplastics,” *Addit. Manuf.*, vol. 36, no. March, p. 101409, 2020, doi: 10.1016/j.addma.2020.101409.
- [4] A. M. et al. Stano, G., Di Nisio, A., Lanzolla, “Fused filament fabrication of commercial conductive filaments : experimental study on the process parameters aimed at the minimization , repeatability and thermal characterization of electrical resistance,” *Int J Adv Manuf Technol*, no. 111, pp. 2971–2986 (2020), 2020.
- [5] A. Maurel *et al.*, “Considering lithium-ion battery 3D-printing via thermoplastic material extrusion and polymer powder bed fusion,” *Addit. Manuf.*, vol. 37, no. July 2020, 2021, doi: 10.1016/j.addma.2020.101651.
- [6] H. Liu, H. Zhang, W. Han, H. Lin, R. Li, and J. Zhu, “3D Printed Flexible Strain Sensors : From Printing to Devices and Signals,” vol. 2004782, pp. 1–19, 2021, doi: 10.1002/adma.202004782.
- [7] H. Watschke, M. Goutier, J. Heubach, T. Vietor, K. Leichsenring, and M. Böhl, “Novel Resistive Sensor Design Utilizing the Geometric Freedom of Additive Manufacturing,” 2021.
- [8] K. Kim, J. Park, J. Suh, M. Kim, Y. Jeong, and I. Park, “Sensors and Actuators A : Physical 3D printing of multi-axial force sensors using carbon nanotube (CNT)/ thermoplastic polyurethane (TPU) filaments,” *Sensors Actuators A. Phys.*, vol. 263, pp. 493–500, 2017, doi: 10.1016/j.sna.2017.07.020.
- [9] M. Maurizi *et al.*, “Dynamic measurements using FDM 3D-printed embedded strain sensors,” *Sensors (Switzerland)*, vol. 19, no. 12, pp. 1–15, 2019, doi: 10.3390/s19122661.
- [10] Arh, Slavič, and Boltežar, “Design principles for a single-process 3d-printed accelerometer – theory and experiment,” vol. 152, 2021, doi: 10.1016/j.ymssp.2020.107475.
- [11] M. Mohiuddin and S. V. Hoa, “Temperature dependent electrical conductivity of CNT-PEEK composites,” *Compos. Sci. Technol.*, vol. 72, no. 1, pp. 21–27, Dec. 2011, doi: 10.1016/j.compscitech.2011.08.018.
- [12] S. W. Kwok *et al.*, “Electrically conductive filament for 3D-printed circuits and sensors,” *Appl. Mater. Today*, vol. 9, pp. 167–175, 2017, doi: 10.1016/j.apmt.2017.07.001.

- [13] F. Daniel, N. H. Patoary, A. L. Moore, L. Weiss, and A. D. Radadia, "Temperature-dependent electrical resistance of conductive polylactic acid filament for fused deposition modeling," *Int. J. Adv. Manuf. Technol.*, vol. 99, no. 5–8, pp. 1215–1224, Nov. 2018, doi: 10.1007/s00170-018-2490-z.
- [14] L. Y. W. Loh, U. Gupta, Y. Wang, C. C. Foo, J. Zhu, and W. F. Lu, "3D Printed Metamaterial Capacitive Sensing Array for Universal Jamming Gripper and Human Joint Wearables," *Adv. Eng. Mater.*, vol. 2001082, pp. 1–9, 2021, doi: 10.1002/adem.202001082.
- [15] A. Rivadeneyra and J. A. L., "Recent Advances in Printed Capacitive Sensors," *Micromachines*, 2020.
- [16] Yang, "Inkjet-printed capacitive sensor for water level or quality monitoring theoretically and experimentally," *Mater. Chem. A*, 2017, doi: 10.1039/C7TA05094A.
- [17] D. Paczesny, G. Tarapata, and R. Jachowicz, "The capacitive sensor for liquid level measurement made with ink-jet printing technology," vol. 120, pp. 731–735, 2015, doi: 10.1016/j.proeng.2015.08.776.
- [18] F. J. Romero *et al.*, "Chemical Design , fabrication and characterization of capacitive humidity sensors based on emerging flexible technologies," *Sensors Actuators B. Chem.*, vol. 287, no. February, pp. 459–467, 2019, doi: 10.1016/j.snb.2019.02.043.
- [19] T. Rahman, A. Rahimi, S. Gupta, and R. Panat, "Physical Microscale additive manufacturing and modeling of interdigitated capacitive touch sensors," vol. 248, pp. 94–103, 2016.
- [20] H. Qin, J. Dong, and Y. Lee, "Fabrication and electrical characterization of multi-layer capacitive touch sensors on flexible substrates by additive e-jet printing," *J. Manuf. Process.*, vol. 28, pp. 479–485, 2017, doi: 10.1016/j.jmapro.2017.04.015.
- [21] G. Percoco, L. Arleo, G. Stano, and F. Bottiglione, "Analytical model to predict the extrusion force as a function of the layer height , in extrusion based 3D printing," *Addit. Manuf.*, vol. 38, no. December 2020, p. 101791, 2021, doi: 10.1016/j.addma.2020.101791.
- [22] A. Dey and N. Yodo, "A Systematic Survey of FDM Process Parameter Optimization and Their Influence on Part Characteristics," *J. Manuf. Mater. Process.*, vol. 3, no. 3, p. 64, 2019, doi: 10.3390/jmmp3030064.
- [23] L. E. Helseth, "Nano Energy Interdigitated electrodes based on liquid metal encapsulated in elastomer as capacitive sensors and triboelectric nanogenerators," *Nano Energy*, vol. 50, no. April, pp. 266–272, 2018, doi: 10.1016/j.nanoen.2018.05.047.
- [24] K. Chetpattananondh, T. Tapoanoi, P. Phukpattaranont, and N. Jindapetch, "Sensors and Actuators A : Physical A self-calibration water level measurement using an interdigital capacitive sensor," *Sensors Actuators A. Phys.*, vol. 209, pp. 175–182, 2014, doi:

Conflict of interests

The authors declare no conflicts of interest.

LIST OF FIGURES:

Figure 1- Design of the coplanar capacitive sensor, in red the flexible substrate and in black the two electrodes (this image refers to the “Uncovered” version).

Figure 2- “Covered” sensor- a) the lateral slide made of flexible thermoplastic polyurethane on which the top coverage will be manufactured is shown, b) final sensor with the 0.3 mm top coverage.

Figure 3- a) Capacitive sensor during the manufacturing process, b) flexibility of the sensor

Figure 4- Manufactured sensors; a) “Uncovered” sensor, before being sealed with adhesive tape and, b) “Covered” sensor with 0.3 mm top TPU cover.

Figure 5- Measurement setup.

Figure 6 - Capacitance vs liquid level of distilled water level. The same scale is used for both x- and y-axis for better visualization and comparison.

Figure 7 – Offset of linear regression curves with respect to the 1st one – distilled water.

Figure 8 - Capacitance vs liquid level of sunflower oil. The same scale is used for both x- and y-axis for better visualization and comparison.

LIST OF TABLES:

Table 1- Process parameters